A R C H I V E S O F M E T A L L U R G Y A N D M A T E R I A L S
Volume 59 2014 Issue 4
DOI: 10.2478/amm-2014-0281

A.N. WIECZOREK*

THE ROLE OF OPERATIONAL FACTORS IN SHAPING OF WEAR PROPERTIES OF ALLOYED AUSTEMPERED DUCTILE IRON PART I. EXPERIMENTAL STUDIES ABRASIVE WEAR OF AUSTEMPERED DUCTILE IRON (ADI) IN THE PRESENCE OF LOOSE QUARTZ ABRASIVE

ROLA CZYNNIKÓW EKSPLOATACYJNYCH W KSZTAŁTOWANIU WŁAŚCIWOŚCI ZUŻYCIOWYCH STOPOWYCH ŻELIW SFEROIDALNYCH AUSFERRYTYCZNYCH CZĘŚĆ I. EKSPERYMENTALNE BADANIA ZUŻYCIA ŚCIERNEGO W OBECNOŚCI LUŹNEGO ŚCIERNIWA KWARCOWEGO ŻELIW ADI

The paper presents the results of the wear tests of alloyed austempered ductile iron performed on a specially designed test rig simulating real operating conditions for chain wheels which were selected for testing due to their complex rolling and sliding form of contact between elements. The chain wheels subjected to tests were operated with the use of loose quartz abrasive and without it. The studies involved the determination of strength and plastic properties, hardness distributions, microstructure and linear wear of the ADI in question considered as a function of the austempering temperature. Based on the results obtained, the following was found: phase transition of austempered ductile iron can take place for combinations typical of industrial applications, a non-linear increase in the wear as a function of the austempering temperature occurs, an increase in the hardness of all the analysed types of ADI takes place during the operation without the presence of abrasive, the phase transition of austenite into martensite in ADI with a lower content of austenite requires higher loads as compared with cast iron containing 40% of austenite.

Keywords: tribology, austempered ductile iron, wear resistance

W pracy przedstawiono wyniki badań zużyciowych stopowych żeliw ausferrytycznych na specjalnie skonstruowanym stanowisku badawczym imitującym rzeczywiste warunki eksploatacyjne kół łańcuchowych, wybranych do testów z uwagi na złożoną toczno-ślizgową postać współpracy elementów. Testowane koła łańcuchowe były eksploatowane z udziałem luźnego ścierniwa kwarcowego i bez niego. W ramach badań wyznaczono właściwości wytrzymałościowe i plastyczne, rozkłady twardości, mikrostrukturę i zużycie liniowe rozpatrywanych żeliw ADI w funkcji temperatury ausferytyzacji. Na podstawie uzyskanych wyników stwierdzono: w skojarzeniach typowych dla zastosowań przemysłowych może dojść do przemiany fazowej ausferytycznych żeliw sferoidalnych, nieliniowy wzrost zużycia w funkcji temperatury ausferytyzacji, zwiększenie twardości wszystkich analizowanych żeliw ADI przy pracy bez udziału ścierniwa oraz zaistnienie przemiany fazowej austenitu w martenzyt w żeliwach ADI o mniejszej zawartości austenitu wymaga oddziaływania wyższych obciążeń w porównaniu z żeliwem zawierającym 40% austenitu.

1. Introduction

Currently, a number of industries, particularly those related to power engineering and mineral extraction, use machines and equipment at risk of damage due to abrasive wear. Companies have high expectations associated with the use of ADIs that offer a number of advantages [1,2,3] as compared with surface hardened alloy steels. One of the most important factors predisposing these materials for the use in harsh operating conditions is that ADIs are resistant to wear almost in the entire cross-section of the cast.

ADIs are used as materials for machines operating in harsh conditions [4], although their use is not very widespread. This may result from a complex manufacturing technology of these materials with a large number of parameters affecting their functional properties.

There are many scientific studies on wear properties of cast irons subjected to an isothermal treatment. Among the most important works it is worth to mention the study by Nili Ahmadabadi et al. [5], in which the authors proved that appropriate isothermal quenching improves mechanical properties and wear resistance of ADI. Nili Ahmadabadi et al. in another study [6] compared wear properties of ADI and grey cast iron with pearlitic matrix containing phosphorus. They found that the wear resistance of ADI was 2.5 times higher than in the case of the grey cast iron. The higher wear resistance of ADI results from the properties of the ausferritic structure containing bainitic ferrite and retained austenite. Boutorabi et al. [7] demonstrated in relation to aluminium-containing ADI that the

* SILESIAN UNIVERSITY OF TECHNOLOGY, FACULTY OF MINING AND GEOLOGY, 2 AKADEMICKA STR., 44-100 GLIWICE, POLAND

wear resistance depends on the combination of the isothermal process temperature and time. Fordyce and Allen [1] found that the wear resistance of ADI in the absence of lubrication was the same as for steel with a high surface hardness.

Schissler et al. [8] and Owhadi et al. [9] showed that a low content of martensite in the microstructure (at a level of 0.1%) has a positive impact on wear properties of cast irons. The martensite observed by these researchers was formed as a result of the transition from austenite with relatively low carbon content in consequence of phase transitions caused by mechanical stresses. Haseeb et al. [10] also proved that the TRIP mechanism is responsible for wear resistance of ADI.

Prasanna et al. [11] and Voight et al. [12] found that the ausferritic microstructure allows obtaining a significant increase in the relative wear resistance. The influence of the morphology of graphite on the wear of cast irons was examined by Zhang et al. [13], Hatate et al. [14] and Ghaderi et al. [15]. These authors indicated a significant impact of graphite on wear properties of ADIs.

Liu Ping and Bahadur [16] compared wear resistance of steel after isothermal quenching process (with the same structure as the ADI matrix) with the wear resistance of ADI. They found that the steel had a higher resistance. They substantiated this fact by a low resistance of graphite to wear processes and by the propagation of microcracks from the spots formed after the destruction of graphite nodules.

The study by PourAsiabi and PourAsiabi [17] investigated the impact of the time and temperature of the isothermal process on the wear, microstructure and hardness of ADIs containing Mn-Ni-Cu-Mo. It was found that the surface hardness was decreased for the time of austempering longer than 90 minutes. The lowest value of wear was observed for the time of austempering equal to 90 minutes.

Kaleicheva [18] investigated the impact of TiN, TiCN and cBN nano-additives on the structure and wear of ADIs. She observed an increase in the wear resistance of cast irons containing nano-additives by 4 to 32% as compared with cast irons without additives.

Myszka and Wieczorek [19] presented results of studies on the impact of the wear process in the presence of corundum abrasive on the properties and microstructure of ductile cast iron with an addition of Cu and Ni subjected to isothermal quenching at 3 different temperatures. After the wear tests have been carried out it was found that the hardest of the three types of cast iron had the best wear resistance, but the strengthening of the surface apparently occurred in the material with the lowest hardness and best plasticity, containing the highest amount of retained austenite.

Myszka and Wieczorek [20] performed wear tests for 34CrNiMo 6 hardened steel and three types of austempered ductile iron containing Mo and Ni. The tests carried out with the use of loose corundum abrasive revealed that the cast iron had properties comparable to the investigated steel. Microscopic evaluation as well as hardness and magnetic measurements showed that considerable strengthening occurred in the surface layer of the austempered ductile iron. For larger loads, it resulted in a higher wear resistance of ADIs than in the case of the steel.

These studies present the results obtained in laboratory conditions for rolling or sliding motion. However, sets of elements mating with one another in the conditions of rolling-sliding motion are frequently used in the industry. Examples of elements working in the conditions of such a motion include gear and chain wheels. The complex nature of the rolling and sliding motion in conjunction with the movement of the abrasive may change the manner of wear of mating elements.

This study starts a series of publications examining properties of ADIs in the conditions of the rolling-sliding motion similar to real operating conditions. Conditions similar to real operating conditions should be understood as a controlled reproduction of factors associated with elements mating, such as the presence of abrasive, the formation of a corrosive environment and its intensification, the action of dynamic forces typical of a given combination, and the action of external forces. In the available literature, there are no studies on properties of ADIs subjected to simultaneous action of multiple destructive processes.

The first part of this study examines the influence of loose quartz abrasive during mating of real elements – a chain wheel and a chain. The chain wheels were made of ADI subjected to isothermal quenching at 4 different temperatures, which resulted in formation of details with different operating properties. The results of the hardness tests were compared with those obtained for the operation without the presence of abrasive. It should be mentioned that in the course of the wear tests, the mating between the chain wheel and the chain was characterized by significant dynamics, despite the absence of external forces.

2. Experimental details

Ductile iron EN-GJS-600-3 (PN-EN 1563) with the chemical composition shown in Table 1 was used for the wear testing. Castings were made in the form of chain wheels with the shape shown in Fig. 1.

TABLE 1
Chemical composition of ductile iron EN-GJS-600 [mass%]

C	***Si***	***Mn***	***S***	***P***
3.50	2.54	0.16	0.013	0.041
Mg	***Cr***	***Cu***	***Ni***	***Mo***
0.047	0.026	0.50	1.40	0.24

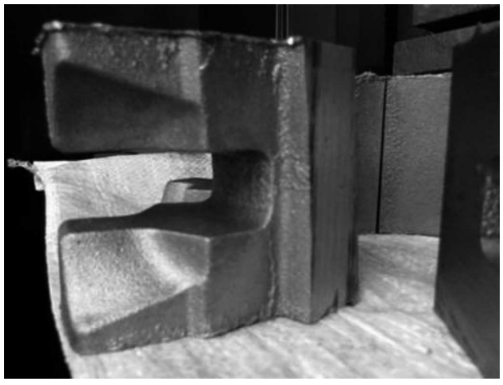

Fig. 1. A view of casting of chain whee

The ductile iron castings had a pearlitic-ferritic structure, a nodule count of 200 graphite nodules per mm^2 and graphite nodularity greater than 90%.

After the necessary operations of cleaning and machining had been carried out, the ductile iron castings were subjected to a heat treatment in order to obtain an ausferritic structure typical for ADIs. The parameters of the austempering and isothermal quenching processes were selected on the basis of previous studies [19,20]. The process parameters are presented in Table 2.

TABLE 2
The process parameters used for the production of samples (chain wheels)

Heat treatment parameters	*ADI_240*	*ADI_270*	*ADI_310*	*ADI_360*
Austenitising temperature,°C	950			
Austenitising time, min	180			
Austempering temperature,°C	240	270	310	360
Austempering time, min	150			

Isothermal quenching was the main process used to produce 4 types of austempered ductile iron. It took place for 150 minutes in a salt bath at 4 temperatures: 240°C, 270°C, 310°C, 360°C. This allowed obtaining castings with different mechanical properties, which were used in the wear tests. After the completion of the austempering process, the castings were cooled in water to remove the salt layer.

The tests of wear properties of ADIs were carried out on a specially designed test rig that allows reproducing the real operating conditions of chain wheels. A schematic diagram of the test rig is shown in Fig. 2.

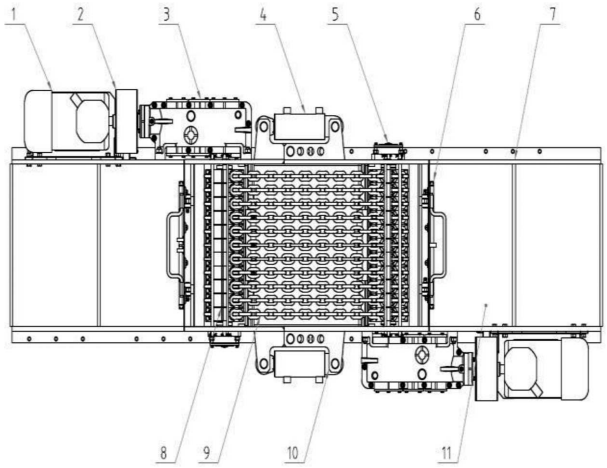

Fig. 2. Schematic diagram of the test rig: 1 – Induction motor 22 kW, 2 – Flexible coupling, 3 – Conical-cylindrical reduction gear, 4 – Hydraulic cylinder, 5 – Axle shaft, 6 – Sprinkler system for the test chamber, 7 – Body of the test rig, 8 – Test samples, 9 – Chain, 10 – Mounting bracket of the hydraulic cylinder, 11 – Additional chamber for aggregate

The impact of the operational factors was reproduced by filling the test box with quartz abrasive, which resulted in its continuous presence between the chain wheels made of ADI and the chain surface.

A diagram of the load generated by the force resulting from the driving torque is shown in Fig. 3.

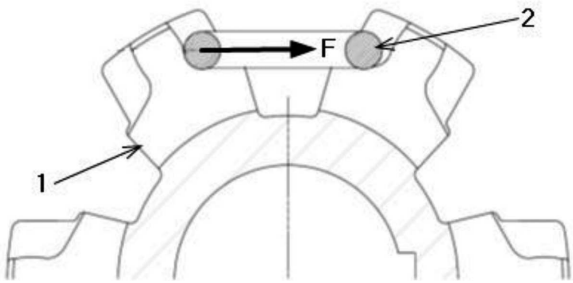

Fig. 3. Load diagram of the sample (chain wheel); designations: 1 – chain wheel, 2 – chain, F – driving force

Load conditions of the test samples were determined directly on the test rig by measuring the power consumed by electric motors using a clamp meter. The determined value of the power consumed by each motor was 7.5 kW (15 kW in total). In a further stage of the analysis, the surface pressure between a chain link and the chain wheel seat was determined. Reduced stress values at the base of the chain wheel tooth were also determined using the FEM method (Fig. 4). Input parameters for the FEM simulation and the stress values determined are presented in Table 3.

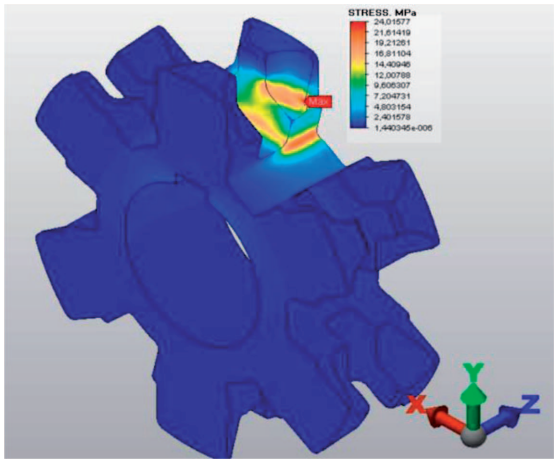

Fig. 4. The results of the FEM simulation used to determine the value of the reduced stress at the base of the chain star tooth

TABLE 3
Input parameters for the FEM simulation and the stress values determined in the chain wheel

Parameters	*Value*
Power consumed by 1 motor, kW	7.5
Gear ratio i,	29.6
Rotational speed, rpm	49.7
Linear speed of the chain, m· s^{-1}	0.7
Peripheral force per 1 contact Ft, N	488.0
Maximum surface pressures, MPa	48.9
Reduced maximum stresses, MPa	2.2

Two sets of the chain wheels (set was composed of four different variants of ADI) with the same functional properties were used for the wear tests. The main wear tests were carried out in the presence of loose quartz abrasive (Fig. 5). They lasted for 200 hours in total: 100 hours for the counter-clockwise direction of both motors and 100 hours for the clockwise direction. The samples designated as ADI_240, ADI_270, ADI_310 and ADI_360 were used for this test cycle.

Fig. 5. A view of the chain wheels during the wear tests in the presence of quartz abrasive

Wheels of the second set (designated as ADI_240_T, ADI_270_T, ADI_310_T and ADI_360_T) were operated for 100 hours (50 hours in the counter-clockwise direction of both motors and 50 hours for the clockwise direction) without the presence of loose abrasive.

After the completion of the wear tests, the microstructure of wheels from both sets was examined, Vickers HV0,1 hardness was determined as a function of the distance from the surface, and the Brinell hardness test was performed in the contact area between the wheel and the chain.

Before the main tests have been started, the area of 24 surfaces of seats of all the chain wheels used in a given test cycle was measured in the area of contact with the chain using the software for the Zeiss Acura measuring machine. A view of a chain wheel during measurements is shown in Fig. 6. Approx. 300 points along a predefined route of the tip of the machine's measuring head were read and recorded during the measurement.

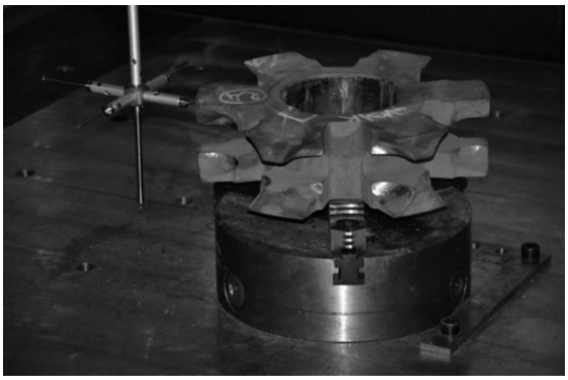

Fig. 6. A view of the castings used for the wear tests during the measurements on the coordinate measuring machine (CMM)

After the completion of the test cycle, the surface of 24 seats of all the chain wheels used in a given test cycle was measured again in the area of contact with the chain. In order to determine the linear wear, the distance δ_i between the i-th measuring point was measured before and after the tests. It is expressed by the following dependence:

$$\delta_{\mathrm{i}} = \sqrt{(\mathrm{x_{i,1}} - \mathrm{x_{i,2}})^2 + (\mathrm{y_{i,1}} - \mathrm{y_{i,2}})^2 + (\mathrm{z_{i,1}} - \mathrm{z_{i,2}})^2} \tag{1}$$

where:

$x_{i,1}$ – *x coordinate of the i-th point before the test,*
$x_{i,2}$ – *x coordinate of the i-th point after the test,*
$y_{i,1}$ – *y coordinate of the i-th point before the test,*
$y_{i,2}$ – *y coordinate of the i-th point after the test,*
$z_{i,1}$ – *z coordinate of the i-th point before the test,*
$z_{i,2}$ – *z coordinate of the i-th point after the test.*

Based on the determined values of wear δ_i, the maximum value for the test surface $\delta_{i,MAX}$ was calculated.

$$\delta_{\mathrm{i,MAX}} = \mathrm{Max}\,\{\delta_{\mathrm{i}}\} \tag{2}$$

The $\delta_{i,MAX}$ values determined for all 24 areas measured for a given wheel were averaged.

$$\delta_{\mathrm{AVR\_MAX}} = \frac{\sum_{1}^{n} \delta_{\mathrm{i,MAX}}}{N} \tag{3}$$

where:

N – the number of surfaces of the seats of the chain wheel (N = 24).

The δ_{AVR_MAX} value was adopted as a measure of abrasive wear for the chain wheel. Apart from the δ_{AVR_MAX} value, the standard deviation S_{δ} and the standard deviation of the average value $S_{\delta x}$ were also determined as a measure of the scatter of results in relation to the average value.

3. Results and discussion

3.1. The structures and characteristics of ADI before abrasion

Together with the castings used for the wear tests, there were produced also Y wedge castings, from which test samples for testing the mechanical properties after the heat treatment were made. The results obtained are summarized in Table 4, while Figures 7, 8 and 9 show plots of the measured values as a function of the austempering temperature.

In Fig. 7 it can be easily noticed that the strength of castings decreases along with an increase in the austempering temperature. This dependence results from an increase in the content of high-carbon austenite along with an increase in the austempering temperature. A similar dependence is illustrated in Fig. 8, where a decrease in the hardness occurs for higher temperatures of the austempering process. In this case, also retained austenite may cause a decrease in the hardness.

TABLE 4
Mechanical properties of the ADIs tested (measurement uncertainty determined for f=N-1=4 and α =0.05)

Mechanical Properties	***ADI_240***	***ADI_270***
Tensile Strength TS, MPa	*1507±4,6*	*1372±4,8*
Yield Strength YS, MPa	*1072±4,4*	*936±4,5*
Impact Toughness K, J	*54±1,1*	*72±1,1*
Elongation A5, %	*3±0,1*	*4±0,1*
Hardness H, HB	*415±4*	*388±4*
Mechanical Properties	***ADI_310***	***ADI_360***
Tensile Strength TS, MPa	*1132,0±3,9*	*1028,1±3,8*
Yield Strength YS, MPa	*804,2±3,6*	*652,0±3,9*
Impact Toughness K, J	*84±1,1*	*124±1,1*
Elongation A5, %	*5±0,1*	*10±0,1*
Hardness H, HB	*331±3*	*283±3*

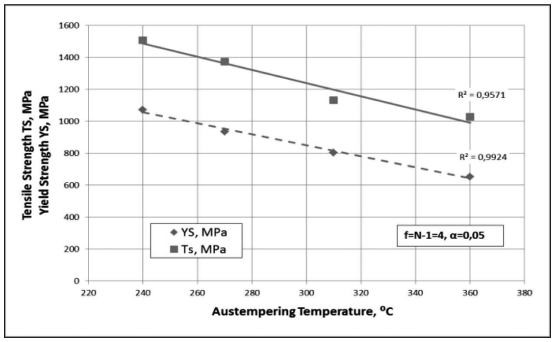

Fig. 7. The maximum strength and the yield strength as a function of the austempering temperature (the maximal measurement uncertainty was 4.8 MPa determined for f=N-1=4 and α =0.05)

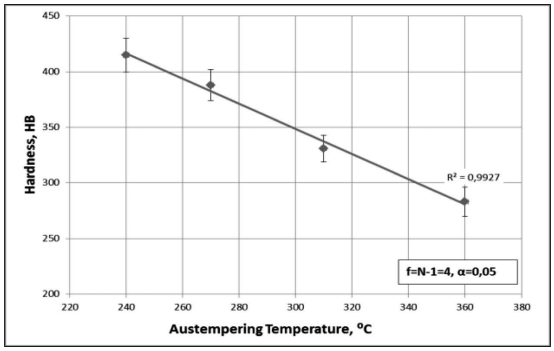

Fig. 8. The HB hardness as a function of the austempering temperature (the maximal relative measurement uncertainty of hardness was 1% determined for f=N-1=4 and α =0.05)

In turn, the increase in the content of austenite causes an increase (Fig. 9) of plastic properties of the castings characterized by the following parameters: impact resistance K and elongation A5.

Guzik [21], Dymski et al., [22] and Dziadur [23] also found that an increase in the austenite content resulted in a decrease in the mechanical strength and hardness as well as in a simultaneous increase in the plasticity of ADI.

The observations of the microstructure were performed using the OLYMPUS X70 optical microscope with 50x – 1000x magnification. Figure 10 presents the microstructure of ADI_240, ADI_270, ADI_310 and ADI_360 cast irons before the wear tests.

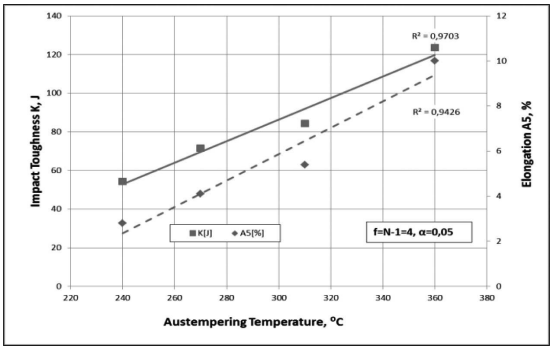

Fig. 9. The impact resistance K and the elongation A5 (the measurement uncertainty of impact resistance was 1.1 J and for elongation was 0.1% determined for f=N-1=4 and α =0.05) as a function of the austempering temperature

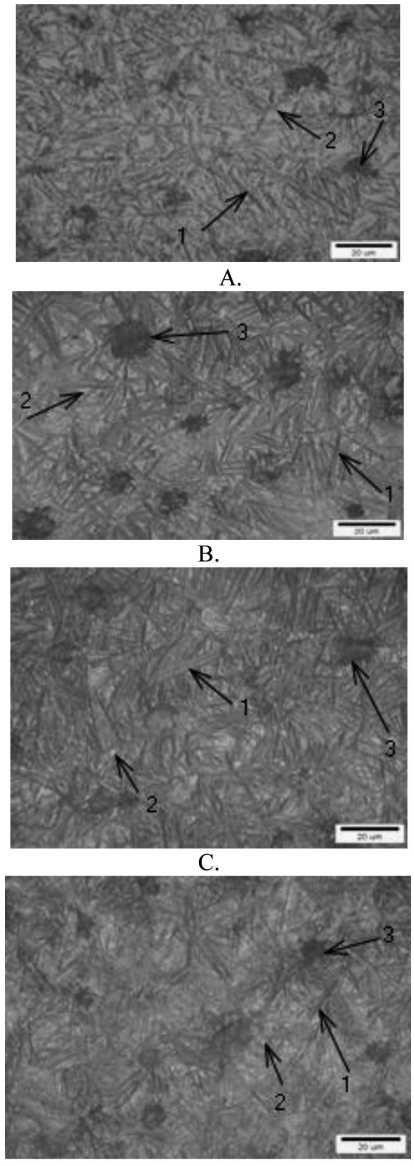

Fig. 10. Microstructure of ADI_360 (A), ADI_310 (B), ADI_270 (C) and ADI_240 (D) cast irons before the wear tests; magnification: 1000x; 1 – bainitic ferrite, 2 – austenite, 3 – graphite

Figure 10A shows the microstructure of ADI isothermally quenched at the temperature of 360°C (ADI_360). Nodular graphite and upper ausferrite composed of bainitic ferrite and stable austenite can be identified in the structure. The total content of austenite was estimated at the level of 40%. Figure 10B shows the microstructure of the cast iron designated as ADI_310. Its structure is also composed of graphite and upper ausferrite, however the content of austenite is 27%. The structure of ADI_270 (Fig. 10C) and ADI_240 (Fig. 10D) consists of nodular graphite and lower ausferrite composed of ferrite, trace amounts of martensite and low-carbon austenite, the content of which was at the level of 20% and 12% respectively.

Figure 11 shows a plot of the content of retained austenite in the ADIs tested as a function of the austempering temperature. A linear dependence between the content of retained austenite and the temperature of isothermal quenching can be seen in this plot.

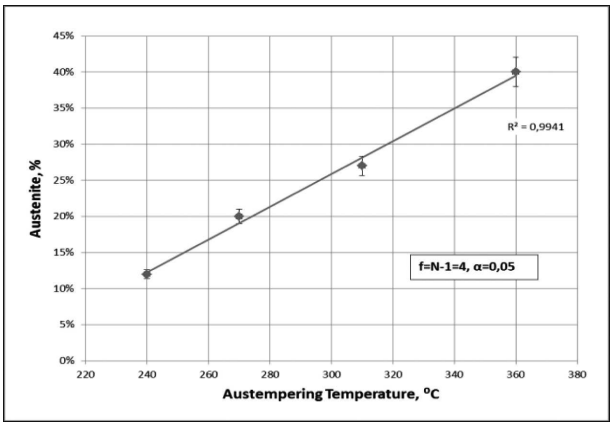

Fig. 11. The austenite content in the test samples as a function of the austempering temperature (the maximal relative measurement uncertainty was 5% determined for f=N-1=4 and α =0.05)

3.2. Results of wear tests without the presence of abrasive

Chain wheels of the second set: ADI_240_T, ADI_270_T, ADI_310_T and ADI_360_T were tested on the wear bench without the presence of abrasive. A rolling and sliding contact typical for chain conveyors occurred between the wheels and the chains. Due to a certain slack of the chain, the operation of the elements in contact was characterized by a variability of the load, which resulted from the mating of the chain with the wheel teeth. This type of the dynamics will be referred to in this study as induced by internal factors.

During the tests of the chain wheels without the presence of abrasive, no traces of abrasion were found and linear wear values were not determined (the uncertainty of the measurement was higher than the linear wear values).

Plots of Vickers HV hardness determined in the area of contact between the wheel and the chain as a function of the distance from the surface are presented in Fig. 12, while values of the maximum hardness HV_{MAX}, core hardness HV_{CORE} and Brinell surface hardness HB surface are listed in Table 5.

Based on Fig. 12 and Table 5, it can be concluded that the hardness of the surface layer decreases along with an increase in the temperature of the isothermal process and thus an increase in the content of retained austenite. The hardness distribution in the cross-section shows a significant variation in the range from 0.02 to 0.5 mm from the surface. Many extremes in this range can be observed, but in each case a local maximum occurs, the value of which is considerably higher than the hardness of the core that is not subject to transitions. This clearly proves the occurrence of phase transitions already in the case of mating without the presence of abrasive. The action of the chain itself, and more precisely its vibrations in the mating area, may induce the transition of retained austenite into martensite. This transition takes place more intensively for variants of this ADI characterised by a higher initial content of austenite. The problem of transition of retained austenite into martensite will be discussed in more detail in the second part of this paper.

TABLE 5

Values of the maximum hardness HV_{MAX}, core hardness HV_{CORE} and Brinell surface hardness HB surface obtained for the chain wheels tested without the presence of quartz abrasive (measurement uncertainty determined for f=N-1=4 and α =0,05)

Designation	HV_{MAX}	HV_{CORE}	*HB*
ADI_240_T	657±7	579±6	391±4
ADI_270_T	560±6	483±5	379±4
ADI_310_T	488±5	429±4	321±3
ADI_360_T	514±5	399±4	277±3

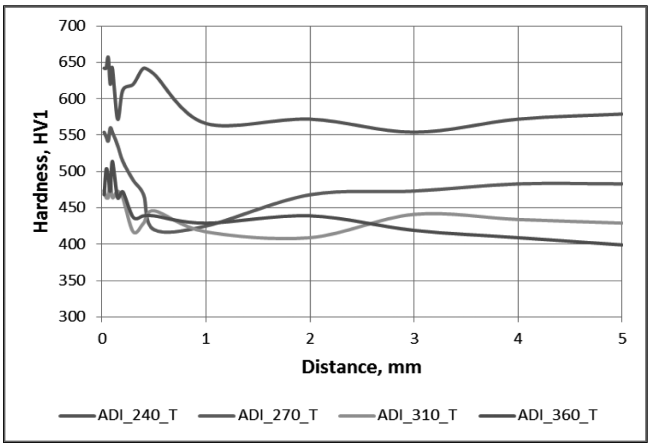

Fig. 12. The Vickers hardness HV0,1 as a function of the distance from the surface of chain wheels operated without the presence of abrasive (the maximal relative measurement uncertainty was 1% determined for f=N-1=4 and α =0.05)

3.3. Results of wear tests in the presence of abrasive

In the first period of wear testing of chain wheels made of ADI conducted in the presence of quartz abrasive (Fig. 5), the abrasive was significantly crushed between mating surfaces of the teeth and the chain. After approx. 10 hours of operation, the intensity of crushing of the abrasive decreased and the size of quartz grains was smaller than 50 μm. As a result of friction between mating elements, the temperature of the chain wheels increased up to 55°C.

The presence of crushed abrasive with a significant hardness intensified the abrasive wear. The leading destructive process was microcutting by loose abrasive (Fig. 13), but no microcutting by the grains fixed to the mating surface was observed. After the completion of the wear test, clear signs of abrasion in the mating surfaces of the tooth and the chain were observed. The abrasions were smooth and shiny (Fig. 14A), while small cavities and scratches could be seen also in some mating areas (Fig. 14B).

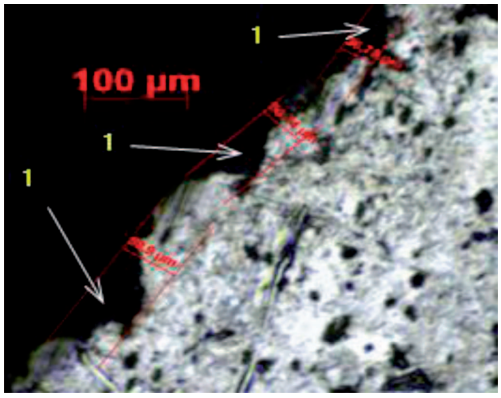

Fig. 13. A view of the microcuts (1) in the abrasion area of ADI_310

A.

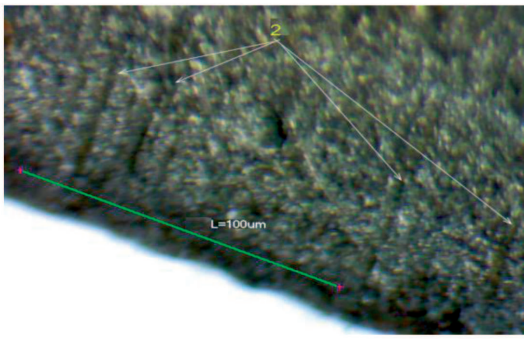

B.

Fig. 14. A view of the area of mating of the chain wheel (ADI_360) with the chain
A. A macroscopic view of the abrasion in the area (1) of mating,
B. A view of scratches (2)

After the shafts had been removed from the test rig, mating surfaces of chain wheels were measured using the coordinate measuring machine and abrasive wear parameters were determined (Table 6). The values determined were presented graphically in Fig. 15 as a function of the austempering temperature.

TABLE 6
The determined parameters characterizing abrasive wear (measurement uncertainty determined for f=N-1=23 and α =0.05)

Designation of sample	δ_{AVR_MAX}, *mm*	S_δ, *mm*	$S_{\delta x}$, *mm*
ADI_360	0.93±0.12	0.28	0.057
ADI_310	0.92±0.10	0.24	0.05
ADI_270	0.80±0.08	0.18	0.037
ADI_240	0.71± *0.08*	0.18	0.037

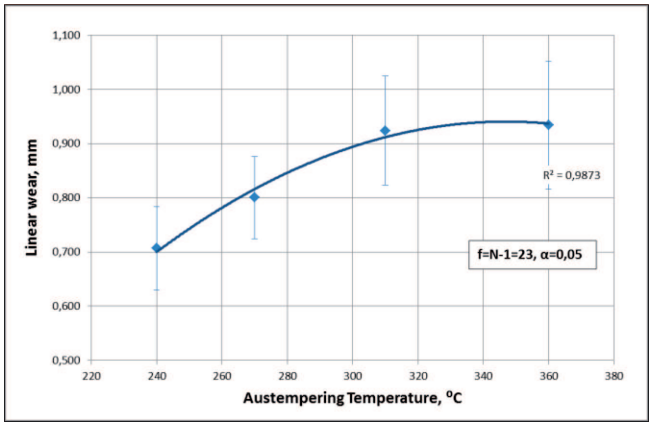

Fig. 15. The wear of test samples as a function of the austempering temperature

After measurements of teeth geometry had been performed, distributions of Vickers hardness HV0,1 were determined (Table 7 and Fig. 16).

TABLE 7
Metallic radii of rare earth metals and magnesium [12]

Designation	HV_{MAX}	HV_{CORE}
ADI_240	772±8	606±6
ADI_270	657±7	536±5
ADI_310	542±5	425±4
ADI_360	525±5	409±4

The plot of wear of the test samples as a function of the austempering temperature (Fig. 15), in contrast to the plots of strength parameters (Fig. 7), hardness (Fig. 8) and plasticity (Fig. 9), does not show linearity, but is described by a second-order polynomial equation. The linear wear values obtained for variants of ADI_310 and ADI_360 are very similar.

The reduction in the wear observed for ADI_360 can be explained by the occurrence of the transition of retained austenite into martensite. The occurrence of the transition is also proved by the Vickers hardness distributions (Fig. 16) obtained for variants of ADI_360 and ADI_310, particularly by similar maximum values of HV_{MAX} (Table 7).

After the wear tests, the samples for metallographic examinations were cut out from the area of mating between the chain wheel and the chain. Then the samples were ground, pol-

ished and etched with a 2% Nital solution. The microstructures obtained are shown in Fig. 17.

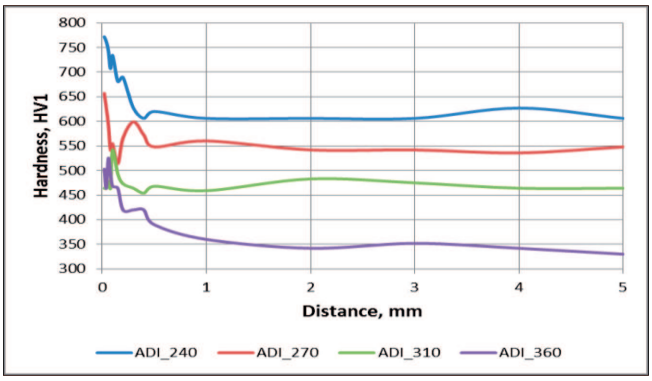

Fig. 16. The Vickers hardness HV0,1 as a function of the distance from the surface of chain wheels operated in the presence of abrasive(the maximal relative measurement uncertainty was 1% determined for f=N-1=4 and α =0.05)

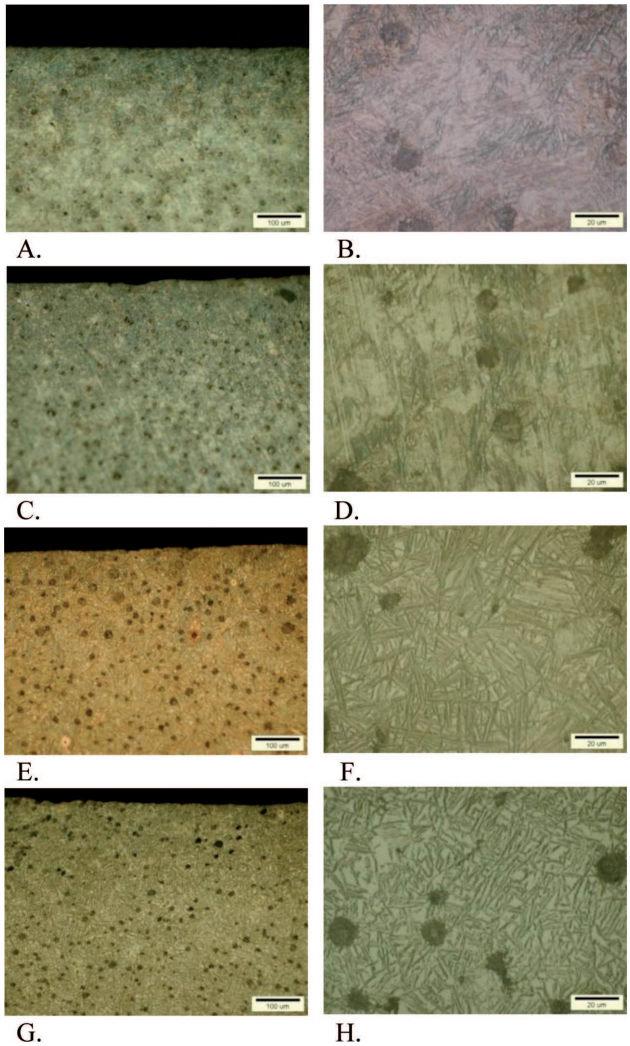

Fig. 17. Microstructure of ADI_240 (A, B), ADI_270 (C, D), ADI_310 (E,F), and ADI_360 (G, H) cast irons after the wear tests

The microstructures at the 1000x magnification are almost identical to those presented in Fig. 10. They confirm the phase composition determined for individual variants of the isothermal treatment, as well as the concentration of austenite. No martensite is observed in this microstructure.

In the case of the ADI_240 variant (Fig. 17A), very shallow oblique cavities caused by abrasion can be seen, while the number of deformed graphite nodules is relatively low. The ADI_270 variant (Fig. 17C) has features very similar to the previous one, but cuts are a bit deeper. The ADI_310 variant (Fig. 17E) is characterized by even deeper cavities as compared with those discussed earlier and by more deformed graphite nodules. There is also a large cavity formed after the area between the two microcuts had crumbled away. Locations of deeper cavities include generally the areas vacated by deformed graphite nodules, which are most exposed to damage. The character of damage to ADI_360 (Fig. 17G) is similar as in the case of ADI_310, but the damage is larger.

Figure 18 shows for all 4 variants of ADI deformed under the pressure of graphite grain.

According to Myszka [32], the most important factor that affects the abrasive wear resistance of the austempered ductile iron is the type of matrix microstructure which depends mainly on austempering parameters. It was found that a harder material with the microstructure consisting of packages of thin ferrite plates separated by stable austenite will require more energy to separate it from the base material during abrasion. A material characterized by higher plasticity and a higher content of austenite (mechanically stable and unstable), strengthened with the participation of deformation transition, will behave similarly. The role of the matrix was confirmed also in the present study.

However, the results of the examinations of the microstructure of the surface clearly indicate the impact of the deformed non-nodular graphite on the intensification of wear. This is confirmed by the research results presented by Al-Ghonamy et al. in their study [33], under which a dependence of the wear on the morphology of graphite was found.

When comparing separately the hardness distributions obtained for chain wheels worn in the presence of abrasive and without it for the variants of austempered ductile iron obtained at the same austempering temperature (Fig. 19), it can be noted that differences in the maximum hardness HV_{MAX} increase along with a decrease in the content of retained austenite. The values determined are summarized in Table 8.

TABLE 8
Comparison of the hardness difference ΔHV_{MAX}

Designation	ΔHV_{MAX}
ADI_240 - ADI_240_T	115
ADI_270 - ADI_270_T	97
ADI_310 - ADI_310_T	54
ADI_360 - ADI_360_T	11

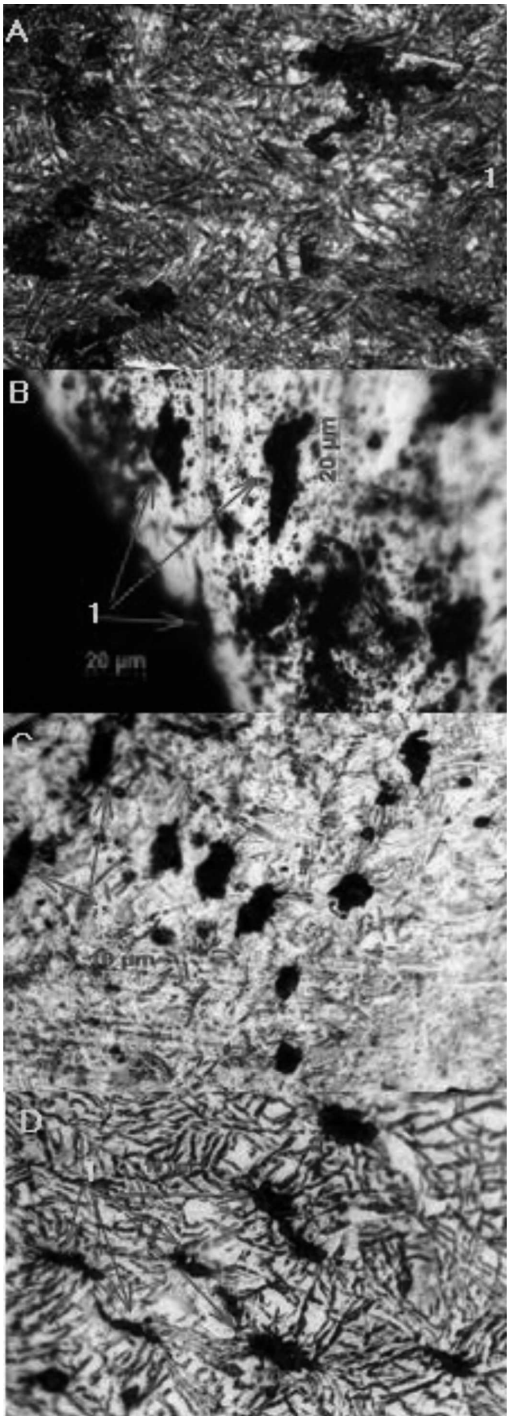

Fig. 18. Deformation of graphite grains (1) in the microstructure of ADI_240 (A), ADI_270 (B), ADI_310 (C) and ADI_360 (D) cast irons in area near the surface

As mentioned above, the mating between the chain wheel and the chain without the participation of abrasive caused significant strengthening of the surface as a result of phase transition of austenite into martensite. A slight difference in ΔHV_{MAX} observed for ADI_360 indicates that almost the entire austenite subjected to the transition in the surface layer was transformed into martensite. The difference in the ΔHV_{MAX} hardness increases along with a decrease in the austempering temperature. This indicates clearly that in the case of ADIs containing less austenite the phase transition requires higher loads caused for example by the action of abrasive on the surface.

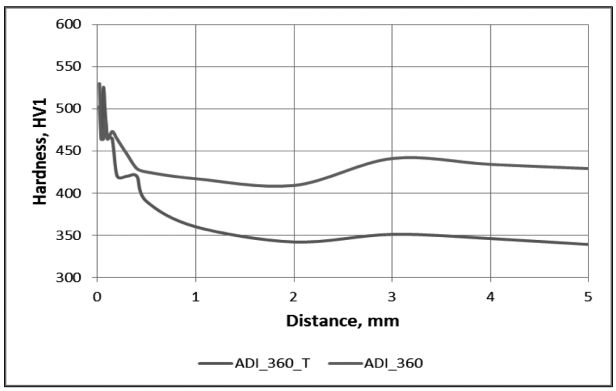

ADI_360 vs. ADI_360_T

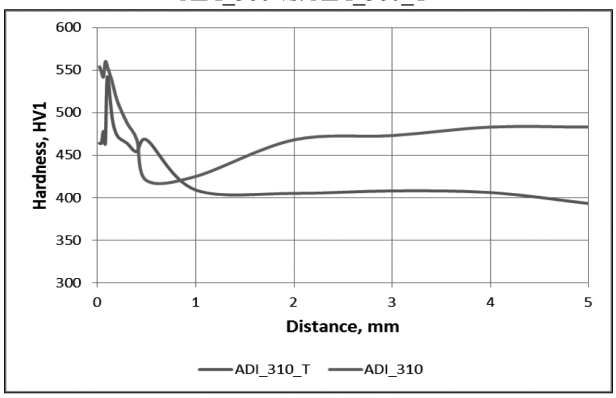

ADI_310 vs. ADI_310_T

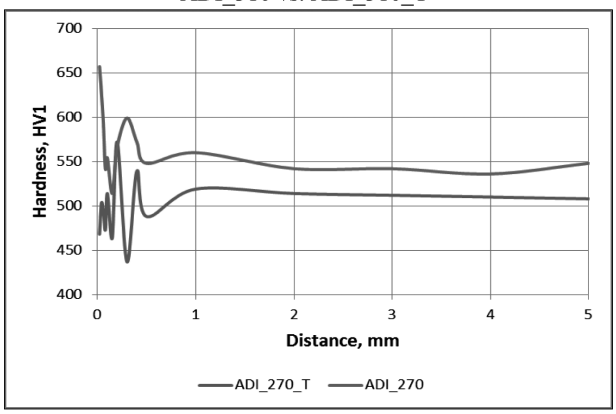

ADI_270 vs. ADI_270_T

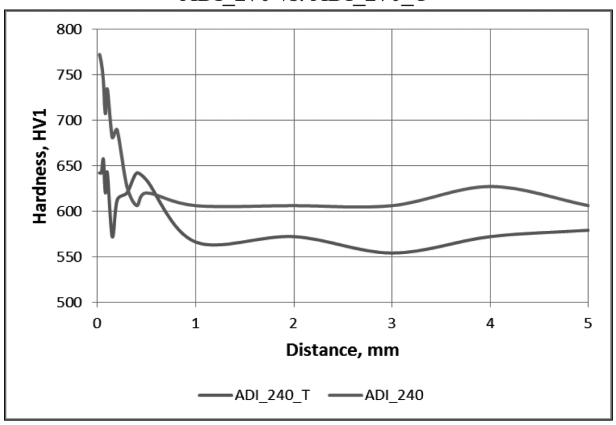

ADI_240 vs. ADI_240_T

Fig. 19. Comparison of plots of Vickers hardness HV0,1 for chain wheels worn in the presence of abrasive and without it

4. Conclusions

1. The study based on the hardness tests proved that in combinations typical for industrial applications a phase transition of austempered ductile iron may take place.
2. Based on tests of chain wheels performed in controlled conditions of abrasive wear, a non-linear increase in the wear as a function of the austempering temperature was found.
3. An observation was made that the wear resistance of the cast iron with the highest content of austenite increased due to the action of the abrasive.
4. An increase in the hardness of all the analysed ADIs was found in the case of the operation without the presence of any abrasive.
5. It was found that the increase in ΔHV_{MAX} hardness of the surface layer of chain wheels subject to wear in the presence of the abrasive and without it was getting greater along with a decrease in the austempering temperature.
6. It was also found that the occurrence of the phase transition of austenite into martensite in ADIs with lower content of austenite required higher loads as compared with cast iron containing 40% of austenite.

Acknowledgements

The study was carried out as a part of the project "Innovative technology for production of tension members for transport systems with the use of cast materials", No. POIG.01.04.00-24-100/11.

REFERENCES

[1] E.P. Fordyce, C. Allen, Wear **135**, 265-278 (1990).
[2] K.L. Hayrynen, J.R. Keough, AFS Transactions **187**, 1-10 (2005).
[3] K.L. Hayrynen, J.R. Keough, G.L. Pioszak, AFS Transactions, 1-15 (2010).
[4] J.R. Brown, Foseco Ferrous Foundryman's Handbook, 11^{th} edition, 95-107, (2000).
[5] M. Ahmadabadi Nili, H.M. Ghasemi, M. Osia, Wear **231**, 293-300 (1999).
[6] M. Ahmadabadi Nili, S. Nategh, P. Davami, Cast Metals **4**, 188-193(1992).
[7] S.M.A. Boutorabi, J.M. Young, V. Kondic, Wear **175**, 19-24 (1993).
[8] J.M. Schissler, P. Brenot, J.P. Chobaut, Mater. Sci. Tech. **5**, 71-77 (1987).
[9] A. Owhadi, J. Hedjazi, P. Davami, Mater. Sci. Tech. **14**, 245-250 (1998).
[10] A.S.M.A. Haseeb, M. Aminul Islam, Wear **244**, 15-19 (2000).
[11] N.D. Prasanna, M.K. Muralidhara, Proc., World Conference on ADI, 456-467 (1991).
[12] R.C. Voigt, R. Bendaly, J.F. Janowak, Y.J. Park, AFS Transactions **93**, 453-462 (1985).
[13] Y. Zhang, Y. Chen, R. He, B. Shen, Wear **166**, 179-186 (1993).
[14] M. Hatate, T. Shoita, N. Takahashi, K. Shimizu, Wear **251**, 885-889 (2001).
[15] A.R. Ghaderi, M. Ahmadabadi Nili, H.M. Ghasemi, Wear **255**, 410-416 (2003).
[16] L. Ping, S. Bahadur, Wear, **138**, 269-284 (1990).
[17] H. PourAsiab, H. PourAsiab, Materials of International Iron & Steel Symposium, Karabük, Türkiye, 616-625 (2012).
[18] J. Kaleicheva, Tribology in Industry **36/1**, 74-78 (2014).
[19] D. Myszka, A. Wieczorek, Material Engineering (Inżynieria Materiałowa) **4/194**, 332-335 (2013.
[20] D. Myszka, A. Wieczorek, Archives of Metallurgy and Materials **58/3**, 967-970 (2013).
[21] E. Guzik, Archiwum Odlewnictwa. Monografia 1M, 1-128, (2001).
[22] S. Dymski, M. Trepczyńska-Łent, Z. Ławrynowicz, Archives of Foundry (Archiwum Odlewnictwa) **6/21**, 125-134 (2006).
[23] W. Dziadur, 11th International Scientific Conference Achievements in Mechanical & Materials Engineering, 179-182.
[24] D. Myszka, Monografia, Prace Naukowe Politechniki Warszawskiej, z. 265 Inżynieria Produkcji (2014).
[25] A.I. Al-Ghonamy, M. Ramadan, N. Fathy, K.M. Hafez, A. A. El-Wakil, International Journal of Civil & Environmental Engineering, **10/3**, 1-5 (2010).

Received: 20 October 2013.